Vol.4, February.2014 ISSN 2354-7065

Journal of Ocean, Mechanical and Aerospace

-Science and Engineering-

ISOMAse

International Society of Ocean, Mechanical and Aerospace, Scientists and Engineers

Journal of Ocean, Mechanical and Aerospace
-Science and Engineering-
Vol.4: February 2014

Contents

ISOMAse

International Society of Ocean, Mechanical and Aerospace
-Scientists and Engineers-

Journal of Ocean, Mechanical and Aerospace
-Science and Engineering-
Vol.4: February 2014

About JOMAse

The **Journal of Ocean, Mechanical and Aerospace -science and engineering- (JOMAse, ISSN: 2354-7065)** is an online professional journal which is published by the International Society of Ocean, Mechanical and Aerospace -scientists and engineers- (ISOMAse), Insya Allah, twelve volumes in a year. The mission of the JOMAse is to foster free and extremely rapid scientific communication across the world wide community. The JOMAse is an original and peer review article that advance the understanding of both science and engineering and its application to the solution of challenges and complex problems in naval architecture, offshore and subsea, machines and control system, aeronautics, satellite and aerospace. The JOMAse is particularly concerned with the demonstration of applied science and innovative engineering solutions to solve specific industrial problems. Original contributions providing insight into the use of computational fluid dynamic, heat transfer, thermodynamics, experimental and analytical, application of finite element, structural and impact mechanics, stress and strain localization and globalization, metal forming, behaviour and application of advanced materials in ocean and aerospace engineering, robotics and control, tribology, materials processing and corrosion generally from the core of the journal contents are encouraged. Articles preferably should focus on the following aspects: new methods or theory or philosophy innovative practices, critical survey or analysis of a subject or topic, new or latest research findings and critical review or evaluation of new discoveries. The authors are required to confirm that their paper has not been submitted to any other journal in English or any other language.

ISOMAse

International Society of Ocean, Mechanical and Aerospace
-Scientists and Engineers-

Journal of Ocean, Mechanical and Aerospace
-Science and Engineering-
Vol.4: February 2014

Scope of JOMAse

The JOMAse welcomes manuscript submissions from academicians, scholars, and practitioners for possible publication from all over the world that meets the general criteria of significance and educational excellence. The scope of the journal is as follows:

- Environment and Safety
- Renewable Energy
- Naval Architecture and Offshore Engineering
- Computational and Experimental Mechanics
- Hydrodynamic and Aerodynamics
- Noise and Vibration
- Aeronautics and Satellite
- Engineering Materials and Corrosion
- Fluids Mechanics Engineering
- Stress and Structural Modeling
- Manufacturing and Industrial Engineering
- Robotics and Control
- Heat Transfer and Thermal
- Power Plant Engineering
- Risk and Reliability
- Case studies and Critical reviews

The International Society of Ocean, Mechanical and Aerospace –science and engineering is inviting you to submit your manuscript(s) to isomase.org@gmail.com or jaswar.koto@gmail.com for publication. Our objective is to inform authors of the decision on their manuscript(s) within 2 weeks of submission. Following acceptance, a paper will normally be published in the next online issue.

ISOMAse

International Society of Ocean, Mechanical and Aerospace
-Scientists and Engineers-

Journal of Ocean, Mechanical and Aerospace
-Science and Engineering-
Vol.4: February 2014

Editors

Published in Indonesia.

JOMAse

ISOMAse,
Jalan Sisingamangaraja No.89
28282, Pekanbaru-Riau
INDONESIA
http://www.isomase.org/

Printed in Indonesia.

Teknik Mesin
Faultas Teknik
Universitas Riau, Indonesia

ISOMAse

International Society of Ocean, Mechanical and Aerospace
-Scientists and Engineers-

Journal of Ocean, Mechanical and Aerospace
-Science and Engineering-, Vol.4

February 20, 2014

Numerical Simulation of Underwater Propeller Noise

Bagheri M.R,[a*], Seif M.S,[a] and Mehdigholi H,[a]

[a)] *Sharif University of Technology, Center of Excellence in Hydrodynamic and Dynamic of Marine Vehicles, Tehran, Iran*

*Corresponding author: mrbagheri@mech.sharif.ir, mrb.bagheri@gmail.com

Paper History

Received: 23-December-2013
Received in revised form: 30-December-2013
Accepted: 10-January-2014

ABSTRACT

Noise reduction and control is an important problem in the performance of underwater acoustic systems and in the habitability of the passenger ship for crew and passenger. Furthermore, sound generated by a propeller is critical in underwater detection and it is often related to the survivability of the vessel. This paper presents a numerical study on noises of the underwater propeller for different performance conditions. The non-cavitating and blade sheet cavitation noise generated by an underwater propeller is analyzed numerically in this study. The flow field is analyzed with finite volume method (FVM), and then the time-dependent flow field data are used as the input for Ffowcs Williams–Hawkings (FW-H) formulation to predict the far-field acoustics. Noise characteristics are presented according to noise sources and conditions. The developed flow solver is applied to the model propeller in uniform inflow. Computed results are shown to be in good agreement with other numerical results. The overall results suggest that the present approach is a practicable tool for predicting cavitation and non-cavitation noise of propellers in far field.

KEY WORDS: *Propeller Noise; FVM; FW-H; Far Field.*

NOMENCLATURE

u_i	Fluid velocity component in the xi direction
u_n	Fluid velocity component normal to the surface f=0
v_i	Surface velocity components in the xi direction
v_n	Surface velocity component normal to the surface
$\delta(f)$	Dirac delta function
$H(f)$	Heaviside function
p_∞	Upstream flow pressure
p_v	Vapor pressure
ρ_l	Fluid density
U_∞	Upstream flow velocity
σ	Cavitation number.

1.0 INTRODUCTION

Acoustics design has been considered as an important character of a modern naval ship by many countries. Rapid development of sonar technology, one of the main approaches for detecting warship, has also made it more important to improve the acoustic characteristics of a modern ship. Sound generated by a propeller is critical in underwater detection, and it is often related to the survivability of the vessels. The propeller generally operates in a non-uniform wake field behind the vessel. As the propeller rotates, it is subjected to unsteady force, which leads to discrete tonal noise, and cavitation. Therefore, underwater propeller noise can be classified into cavitating and non-cavitating noise. Cavitation of the underwater propeller is the most prevalent source of underwater sound in the ocean and it is often the dominant noise source of a marine vehicle. In the past, the propeller design philosophy has been avoiding cavitation for the widest possible range of operating conditions. However, the recent demands for high vehicle speed and high propeller load have made this designing philosophy practically impossible to achieve. Therefore, underwater propeller cavitation has been more and more common in recent ocean vehicle application[1]. So both cavitating and non-cavitating noise are also important. The approach for the investigation of the underwater propeller noise is a potential-based panel method coupled with acoustic analogy. Among the various types of cavitation noise, unsteady sheet cavitation on the suction surface is known to produce the highest noise level[2]. Propeller produces pressure waves through four mechanisms [2]:

1. Displacement of water by the rotating blades of the propeller.
2. The pressure difference between the suction and pressure

surfaces of the propeller.
3. The volume fluctuations occurring on the blades that are induced by pressure drop in front and behind of the propeller (there are sheet cavitation on the blades).
4. The process of growth and collapse of sheet and cloud cavitation.

The first two causes occur for cavitating and non-cavitating states, but they are non-cavitating effects only. The latter two occur only when the propeller is experiencing cavitation [2].
Since the cavitation noise is the major source of noise of the propeller it should be analyzed accurately. The general noise spectrum of a cavitating propeller is depicted in Figure 1. The frequency range of sheet cavitation is from 10 Hz to more than 10 kHz. The low frequency noise that form the regions I and II in Figure1 is a result of sheet cavitation and appears as large bubbles on the surfaces of the blades [3].

Sharma et al. [4] have studied some marine propellers in cavitation tunnel. In their study, the difference of Sound Pressure levels (SPLs) in two states of cavitating and non-cavitating conditions is in the range of 10 to 30 dB. In this paper, the amplitude difference in the SPLs, before and after the development of cavitation in a specified center frequency, is approximately in the range of 10 to 30 dB.

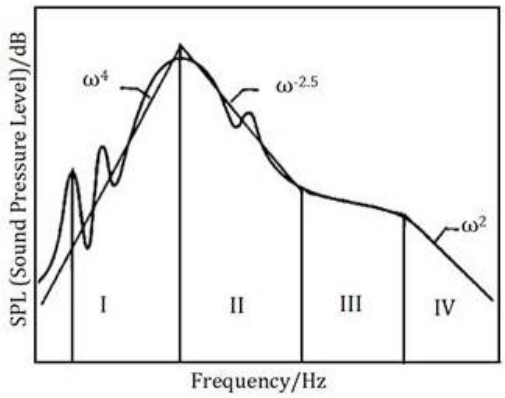

Figure 1: The frequency range of cavitation noise for marine propellers [3].

Jin-Ming et al. in 2012 investigated the noise of a three-blade propeller and concluded that the overall spectrum amplitude of sound in front of the propeller hub exceeds the propeller rotating plane [5]. Bagheri et al. in 2012 and 2013 investigated the non-cavitating/cavitating noise and hydrodynamics of marine propellers using FVM [6-8]. In this work, we used the same modeling approach, turbulence model and numerical solution method [6-8].

This paper presents a numerical study on noises of the underwater propeller for different performance conditions. The non-cavitating and blade sheet cavitation noise generated by an underwater propeller is analyzed numerically in this study. The noise is predicted using time-domain acoustic analogy. Hanshin Seol and eat al. presents a numerical study on the non-cavitating and blade sheet cavitation noises of the underwater propeller [3]. A brief summary of numerical method with verification and results are presented. The noise is predicted using FW-H formulations.

The marine propeller in its non-cavitating statue, in keeping with other forms of turbo-machinery, produces a noise signature of the type sketched in Figure 2. It is seen from this figure that there are distinct tones associated with the blade frequencies together with a broad-band noise at higher frequencies. The broadband noise comprises components derived from inflow turbulence into the propeller and various edge effects such as vortex shedding and trailing edge noise [2].

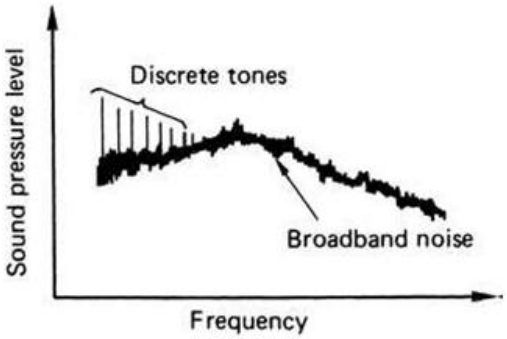

Figure2: Idealized non-cavitating noise spectrum [2].

There are various ways to evaluate Ffowcs Williams–Hawkings equation and the three types of noise source terms (monopole, dipole, and quadrupole) proposed [3]. Farassat proposed a time-domain formulation that can predict noise from an arbitrary shaped object in motion without the numerical differentiation of the observer time [9]. The implementation of this formulation is quite straightforward because contributions from each panel with different retarded times are added to form an acoustic wave. The quadruple noise source term is neglected in this study since the rotating speed of the propeller is much lower than the speed of sound in water. Through these studies, the dominant noise source of underwater propeller is analyzed. Arazgaldi and et al. present RANS simulations of flow around two different conventional propellers were carried out at non-cavitating and cavitating operating conditions using the multiphase flow model based on the “full cavitation model” proposed by Singhal et al [10]. In present paper the flow field is analyzed with finite volume method (FVM), and then the time-dependent flow field data are used as the input for Ffowcs Williams–Hawkings formulation to predict the far-field acoustics. Noise characteristics are presented according to noise sources and conditions. The developed flow solver is applied to the model propeller in uniform inflow.

2.0 METHODOLOGY

2.1 Numerical simulation

In this paper, one type propeller model of Gown series was used for investigations. The geometries and surface grids on the blade and hub surface of the propeller model are shown in Figure 3 and Table 1, respectively.

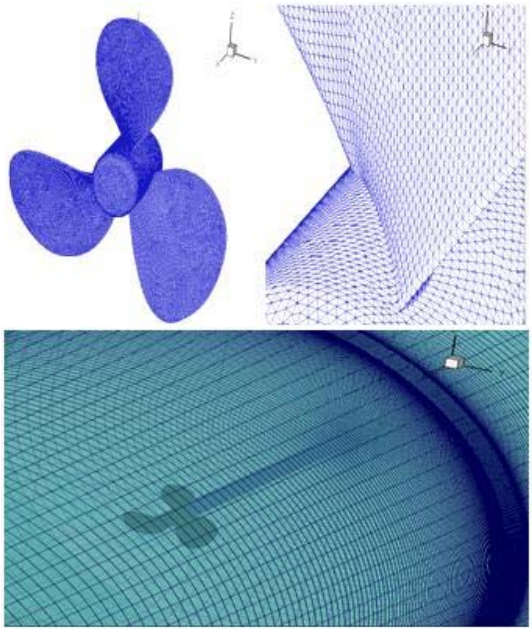

Fiugure3: Propeller 3D model and mesh grids.

Table 1: Principal particulars of propeller model.

Diameter (m)	0.3m
EAR= A_E/A_0	0.5
N. of Blade	3
Hub ratio	0.2
Series	Gown

Computational methods for cavitation flows can be largely categorized into two groups: single-phase modeling with cavitation interface tracking and multi-phase modeling with an embedded cavitation interface. The former approach has been widely adopted for inviscid flow solution methods and Euler equation solvers. In this paper is used of multi-phase model.

The cavitation model employed in the present study was introduced by Singhal et al. [12]. This model is based on multiphase flows and has the capability of accounting for the effects of slip velocity between liquid and gaseous phases. The main part of every cavitation physical model is to find the mass transfer equation between the liquid and vapor phases. In the present study, we used the following equation [12]:

$$\frac{\partial(\alpha_l\rho_l)}{\partial x} + \nabla\cdot(\alpha_l\rho_l C_m) = \Gamma_n = \dot{m}_l^v + \dot{m}_c^v \qquad (1)$$

In solving equation (1), α_l, ρ_l are the volume fraction and the density of liquid, respectively. $\dot{m}_l^v$, $\dot{m}_l^c$ are to be related to the bubble dynamics and vapor volume fraction that they defined the source terms for transfer equation. To account for the bubble dynamics, the reduced Rayleigh-Plesset equation is employed for source terms in transfer equation. The expression for $\dot{m}_l^v$, $\dot{m}_l^c$ are obtained as:

$$\dot{m}_l^v = -F^v \frac{3\rho_v\alpha_{nuc}\alpha_l}{R_0}\sqrt{\frac{2}{3}Max\left(\frac{P_v-P}{\rho_l},0\right)} \qquad (2)$$

$$\dot{m}_c^v = -F^c \frac{3\rho_v(1-\alpha_l)}{R_0}\sqrt{\frac{2}{3}Max\left(\frac{P_v-P}{\rho_l},0\right)} \qquad (3)$$

In equations (2) and (3) F^v *and* F^c are two empirical constants and Singhal et al. [12] used 0.01 and 50 for F^v *and* F^c, respectively. α_{nuc} is the volume fraction of non-condensing gases, ρ_v is the density of water vapor, p_v is the saturate pressure of water vapor and p is the flow pressure.

The main parts of the numerical simulation of any geometry are kind, size and the meshing quality, such that their compositions severely convergence / divergence and the convergent time of the problem under consideration. First, the blade surface is meshed with triangles [6-8]. The region around the root, tip and blade edges is meshed with smaller triangles, i.e. with sides of approximately 0.005 D. The inner region is filled with triangles of approximately increased size and with aspect ratios of 1.05 and 1.1. In order to resolve the boundary layer on the solid surfaces, four layers of prismatic cells with a stretching ratio of 1.1 are grown from the blade and hub surfaces.

Finally, the remaining region in the domain is filled with tetrahedral cells. Flow domain around propeller and hub set is divided two parts, first part is called moving zone and second part is called stationary zone. The propeller computational domain is cylindrical shape surrounding the propeller where a rotational cylinder with sufficient larger diameter than the propeller diameter enfolds the propeller in its cross section center and allows the fluid to pass by the model. The rotating zone was solved via Moving Reference Frame (MRF) [6-8].

The inlet is 4D upstream; the outlet is 10D downstream; solid surfaces on the blades and hub are centered at the coordinate system origin and aligned with uniform inflow; and the outer boundary is 5D from the hub axis [6-8]. The computational domain for propeller model is shown in Figure 4.

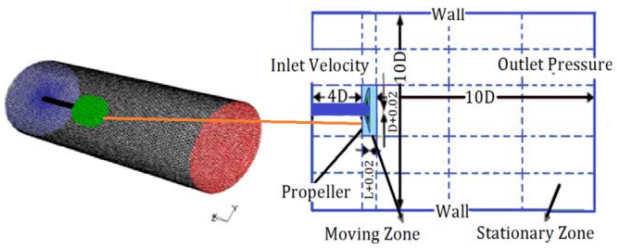

Figure 4: Computational domain around propeller (moving zone and stationary zone) and boundary conditions.

In order to simulate the flow around a rotating propeller, the boundary conditions are as flowing:
On the inlet boundary, velocity components are imposed for a uniform stream with a given inflow speed; on the blade and hub surface, a no slip condition is imposed; on the lateral boundary, a slip boundary condition is imposed; and on the outlet boundary, the pressure is set to a constant value[6-8].

Table 2: Different parameters of flow and acoustic conditions.

statue	Va (m/s)	N (rpm)	turbulence model	ρ(kg/m^3)	a_0 (m/s)	P_{ref} (Pa)
1	3	120	RSM	1025	1500	10^{-6}
2	5	250	RSM	1025	1500	10^{-6}

In table (2), N is rotational speed, Va is axial velocity of flow, ρ is density of water, a_0 is sound velocity and P_{ref} is reference pressure in underwater.

In this Numerical simulation six Hydrophones is used for extraction Sound Pressure Levels (SPLs). The Position of Hydrophones and their coordinates are shown in Figure 5 and Table 3, respectively. Typically in the case of a three-blade propeller operating at say 120rpm this gives a blade rate frequency of 6Hz and operating at say 250rpm this gives a blade rate frequency of 12.5Hz according equation(4), which is just below the human audible range of about 20 to 20 000 Hz [2].

$$f_m = mnf_r \tag{4}$$

Where:
m = harmonic number
n = number of blade
f_r = rotational frequency of the propeller

Table 3: Coordinates of Hydrophones.

Name	X-Coord.(m)	Y-Coord.(m)
Hydrophone 1	0.3	0.15
Hydrophone 2	0.5	0.2
Hydrophone 3	1.5	0.15
Hydrophone 4	0.3	0
Hydrophone 5	0.5	0
Hydrophone 6	1.5	0

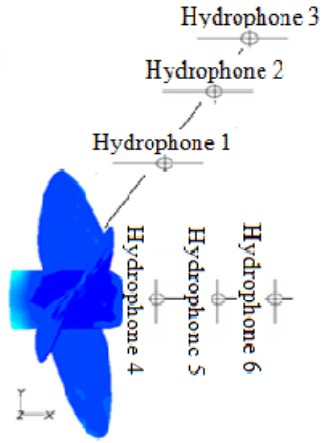

Figure 5: Position of Hydrophones for Numerical simulation.

3.0 RESULT AND DISCUSSION

3.1 Equations and Mathematical Expression

Noise prediction can be represented as the solution of the wave equation if the distribution of sources on the moving boundary (the blade surface) and in the flow field is known. FW-H formulated the following equation for the manifestation of acoustic analogy proposed by Light hill [9]:

$$\frac{1}{{a_0}^2}\frac{\partial^2 p'}{\partial t^2} - \nabla^2 p' = \frac{\partial^2}{x_i x_j}\left[T_{ij}H(f)\right] - \frac{\partial}{\partial x_i}\left(\left[P_{ij}n_j + \rho u_i(u_n - v_n)\right]\delta(f)\right) + \frac{\partial}{\partial t}\left([\rho_0 v_n + \rho(u_n - v_n)]\delta(f)\right) \tag{5}$$

$\acute{p}$ is the sound pressure at the far field ($\acute{p} = p - p_0$). $f=0$ denotes a mathematical surface introduced to "embed" the exterior flow problem (f>0) in an unbounded space, which facilitates the use of generalized function theory and the free-space Green function to obtain the solution. a_0 is the far-field sound speed, and T_{ij} is the Light hill stress tensor. The flow field is analyzed with finite volume method (FVM), and then the time-dependent flow field data are used as the input for FW-H formulation to predict the far-field acoustics.

3.2 Results for two different performance conditions

The cavitation number in each region of the blade was calculated using Equation (6) and (7). If the rotational speed of the propeller was low, the cavitation would be investigated at the root of the propeller *(r= 0)*, while the cavitation would be investigated at *r= 0.7R (R is the radius of blade (m))* [2] for higher speeds.

$$\sigma_{r=0} = \frac{P_0 - P_v}{0.5\rho V_a^2} \tag{6}$$

$$\sigma_{r=0.7R} = \frac{P_0 - P_v}{0.5\rho V_R^2} \tag{7}$$

V_a and $V_R = \sqrt{V_a^2 + (0.7Rw)^2}$ are velocities at $r= 0$ and $r= 0.7R$, respectively. w is the rotational speed of propeller *(rad/s)*. ρ is the water density *(kg/m^3)*. P_0 and P_v are the static pressure and water vapor pressure *(pa)*, respectively.

The contours of flow velocity and flow pressure are shown in Figures 6 and 7, respectively. According to maximum and minimum flow pressure, the cavitation number for first statue shown in Table 4. Sound Pressure level (SPL) for first and sixth Hydrophones are show in Figures 8 and 9, respectively.

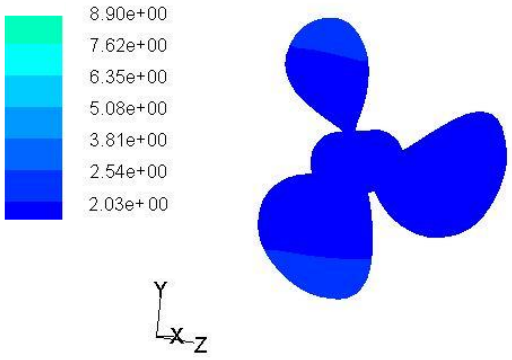

Figure 6: flow velocity contour [m/s] (V_a =3m/s , N=120rpm).

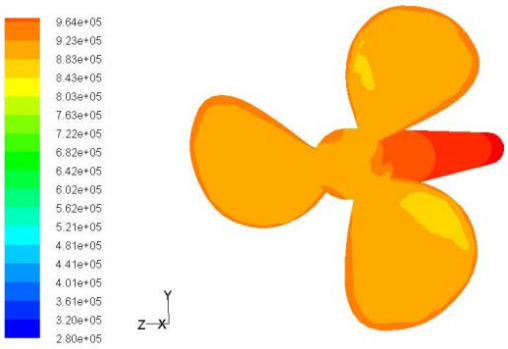

Figure 7: Flow pressure contour (pa) (V_a =3m/s, N=120rpm).

Table 4: Amount of cavitation number for first statue (for numerical and theory solve).

max and min σ for numerical simulation(v=3m/s , w=120rpm)	
max and min σ by theory formulation(v=3m/s , w=120rpm)	
error(v=3m/s , w=120rpm)	
max and min σ for numerical simulation(v=5m/s , w=250rpm)	

Flow solve for second statue show that cavitation number is too lower than first statue. The Contours of flow velocity and flow pressure are shown in Figures 10 and 11, respectively. According to maximum and minimum pressure of flow amount of cavitation number for second statue, is shown in Table 4. The SPL for first and sixth Hydrophones are show in Figures 12 and 13, respectively.

What can be harvested from figures 8, 9, 12 and13 amount of the SPL in second statue is more than first statue. In second statue with increase of flow velocity and rotational speed, flow on blade surface is closed to inception sheet of cavitation. Increase in distance of propeller results increase sound pressure levels (SPLs) which is observed clearly in figures 8 and 9 or 12 and 13.

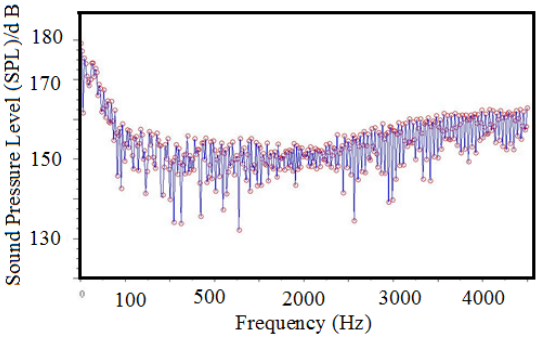

Figure 8: Sound pressure level for hydrophone 1 (V_a =3m/s, N=120rpm).

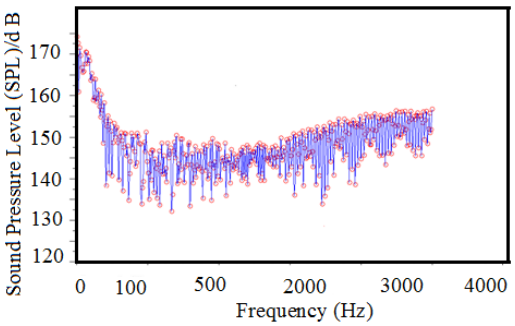

Figure 9: Sound pressure level for hydrophone 6 (V_a =3m/s, N=120rpm).

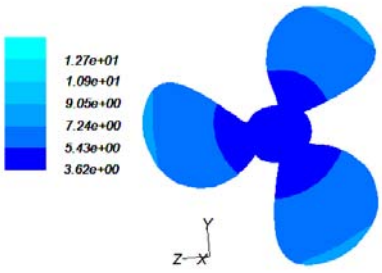

Figure 10: Flow velocity contour (m/s) (V_a =5m/s, N=250rpm).

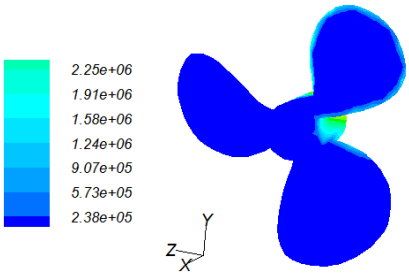

Figure 11: Flow pressure contour (pa) (V_a =5m/s, N=250rpm).

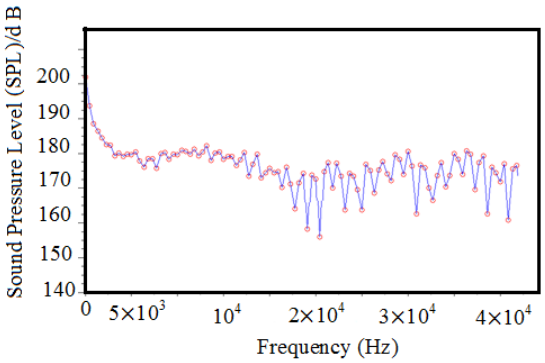

Figure 12: Sound pressure level for hydrophone1 (V_a=5m/s, N=250rpm).

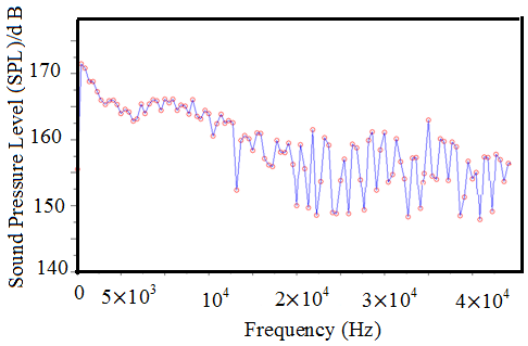

Figure 13: Sound pressure level for hydrophone 6 (V_a =5m/s, N=250rpm)

5.0 CONCLUSION

In this paper, different operating conditions of a propeller model was studied in order to find the ranges of the cavitation initiation and its development and to study the effect of cavitation on the SPLs.

The non-cavitating and blade sheet cavitation noise generated by an underwater propeller is analyzed numerically in this study. The flow field is analyzed with finite volume method (FVM), and then the time-dependent flow field data are used as the input for Ffowcs Williams–Hawkings formulation to predict the far-field acoustics. Noise characteristics are presented according to noise sources and conditions. According to results cavitation going to incept by increase of flow velocity and propeller revolution speed.

In present working two statue velocity and revolution speed was performed which second the statue closed to inception cavitation without cavitiation occurrence so calculated noise in this paper is due to dipole and quaderpole source in light hill equation. With inception cavitation, dominate source of noise is monopole noise which is due to initiation and development of cavitation.

Numerical analysis based on theory provides a basis for cavitation study and scaling of experimentally measured data.

Since hydrophone 1 is located near sound source, the overall SPL for hydrophone 1 is more than hydrophone 6. When the pressure decreases, the cavitation initiation develops. As can be seen from results ranges of SPLs increase with increasing rotational speed of propeller.

The results showed that in the process of initiation of cavitation formation, the increasing effect of rotational speed of propeller was stronger than flow velocity.

The obtained results can be used to optimize the experimental parameters of derivated patterns of noise radiation.

REFERENCE

1. Ross, D. (1976). Mechanics of Underwater Noise Pergamon Press.
2. Carlton, JS. (1994). Marine Propellers and Propulsion, *Butterworth Heinemann, London.*
3. Seol, H., Jung, B., Suh, JC., Lee, S. (2005). Development of hybrid method for the prediction of underwater propeller noise, *J Sound and Vibration 228: 345-360.*
4. Sharma, S.D., Mani. K., Arakeri V.H. (1990). Cavitation Noise Studies on marine propellers, *J Sound and Vibration 138(2): 255-283.*
5. Jin-ming, Y., Ying, X., Fang, L., zhan-zhi, W. (2012). Numerical prediction of blade frequency noise of cavitating propeller, *J Hydrodynamics* 24(3): 371-377.
6. Bagheri, M.R., Seif, M.S., Mahdigholi, H. (2013) Hydrodynamic and acoustic analysis of underwater propellers by numerical method (in Iran), *International Journal of Maritime Technology.*
7. Bagheri, M.R., Seif M.S., Mahdigholi, H. (2012). Numerical Simulation of underwater propeller noise (in Malaysia), *Proceeding of 12th International Conference on Marine Technology, Kuala Terengganu, Malaysia.*
8. Bagheri, M.R., Seif, M.S., Mahdigholi, H. (2012). Numerical simulation of underwater propeller non-cavitating noise by FVM method (in Iran), *Proceeding of 2nd International conference on Vibration and Acoustic*, Iran, Sharif University of Technology.
9. Light hill, MJ. (1952). on sound generated aerodynamically. I. General theory, *Proc, R. Soc. Lond,* vol. 211 no. 1107 564-587.
10. Arazgaldi, R., A. Hajilouy, B. Farhanieh (2009). Experimental and Numerical Investigation of Marine Propeller Cavitation. Sharif University of Technology, *Journal SCIENTIA IRANICA,* Vol. 16, No. 6, pp. 525-533.
11. Ffowcs Williams, JE., Hawkings ,DL. (1969). Sound generated by turbulence and surfaces in arbitrary motion, *Philosophical Transactions of the Royal Society A 264 (1151) 321–342.*
12. Singhal, A.K., Athavale, M.M., Li H., Jiang, Y .(2002). Mathematical basis and validation of the full cavitation model, *ASME J. Fluids Eng, pp. 617-624.*

Journal of Ocean, Mechanical and Aerospace
-Science and Engineering-, Vol.4

February 20, 2014

Occupational Safety in Production of Traditional Fishing Vessels in Indonesia

Jaswar Koto,[a,b,*], Munirah,[a] and Dodi Sofyan Arief,[c]

[a)]*Department of Aeronautical, Automotive and Ocean Engineering, Faculty of Mechanical Engineering, Universiti Teknologi Malaysia*
[b)]*Ocean and Aerospace Engineering Research Institute, Indonesia*
[c)]*Mechanical Engineering, Universitas Riau, Indonesia*

*Corresponding author: jaswar.koto@gmail.com

Paper History

Received:15-November-2013
Received in revised form: 25-November-2013
Accepted: 16-January-2014

ABSTRACT

Traditional ship in Indonesia which usually built from wood has small capacity compared to modern steel ship. Compared to modern ship building, mostly the production is to assemble block by block with machines and big cranes. However, traditional ship is one hundred per cent made from the work of man. Workers are not properly trained in a formal engineering school but only learnt the skill from senior workers. Hence, all modern concepts such as the need for safety and a proper ship production flow are not a great concern for them. In this paper, safety issue in traditional ship production process is being observed conducting direct survey to traditional shipbuilding company in Bintan, Indonesia. It is hoped that the outcome is to bring safety awareness to the traditional ship builders.

KEY WORDS: *Traditional Ship; Equipment; Traditional Ship Production Process, Occupational Safety*.

1.0 INTRODUCTION

Occupational health and safety is a discipline of area that concerns on safety and health of people at workplace. It stands out act called as OSHA which covers on prevention steps, condition, contributing factors to safety issues and also legal consequences of disobedient.

In Indonesia, legal basis which regulating occupational safety is law No.1 1970. On this law regulates about occupational safety in any workplace, whether on land, underground, in water or in the air which are in jurisdiction area of Republic of Indonesia. Several common hazard types such as chemical, physical and safety were covered under OSHA. The laws recommend and taught employers on prevention, securing and healing in the case if accident happened.

This paper intended to analyze the safety issue in the traditional ship production process. The survey was conducted by interviewing traditional shipbuilding company owner directly in Bintan Island, Indonesia. Objective of the study is to observe and to indicate the level of safety applied by traditional shipbuilding workers during working period. By the end of this study, it is expected that awareness of safety and the implementations on safety acts will be successful among the workers.

2.0 LITERATURE REVIEW

There are several institutions of higher education, particularly in Indonesia, doing research on traditional shipbuilding, such as the Bogor Agricultural Institute. Arofik (2007) and Umam (2007) focused in redesigning and the construction process of traditional paying ship in Pemakasan, Madura Indonesia.

Other researchers from other higher education institutions also conducted the study in the same field. Aji (2000) from University of Cendrawasih, Indonesia conducted research on local knowledge of traditional boat building by Biak tribe in the Warsa district Biak Numfor regency with descriptive methods of data collection through a structural interview technique. Putri (2009) from University of Indonesia conducted a research on risk management of Phinisi shipbuilding in project implementation. The study used descriptive research methods and approaches based on risk

analysis through surveys, observations and interviews.

Maidin (2003) studied the institution of boat-building by covering the way Malay boat-builders acquire knowledge, polish skills, organize their work, and the differences they show in their work, based on an in-situ observation and on interviews with boat-builders in Terengganu. Followed by Salam and Katsuya (2008) analyzed the transformation process of wooden boats in the second half of the twentieth century, in which modern technology played an important role, in order to understand the technological adaptation of the local people to the changing situation. E. Prayetno. et.al (2012) and Mufti F.M.et.al (2012) studied quality and design issues of Indonesian traditional ships, respectively.

3.0 OCCUPATIONAL SAFETY IN TRADITIONAL SHIP CONSTRUCTION

In the provinces of Kepulauan Riau, most of ship production industry holds by traditional format of working which explains the design drawing, ship performance calculations, shipyard layout, the production flow, the ship birthing and other requirements during ship production. Workers are trained to master up the skill of using traditional tools and equipment. The only goal of traditional ship building concept is to have the ship to be able to operate at the sea. In the perspective of current regulations, the concept of working carried out by the islands ship builders are rejected as it not satisfying and contradict to safety factors.

3.1 Indonesian Traditional Shipyard Layout

Kepulauan Riau is one of provinces in Indonesia which is an archipelago area consisting of large and small islands around 2.408 islands. 366 of the islands have been inhabited and 2.402 islands have not been yet. Kepulauan Riau Province dwelled upon earth about 253.420 km^2which consisting 242.825 km^2 (96%) of sea and 10.595,41 km^2 (4%) is land, as shown in Figure.1.

Current research aims to promote a better understanding production process of traditional ship in Kepulauan Riau, Indonesia related to safety issues. As case study, the research carried out by visiting three wooden shipbuilders as follows: Kijang-Bintan Island, Kelong Island and Mana Island in Kepulauan Riau, Indonesia as shown in figure 1. All information and data are collected through interview and documentation.

Traditional shipyard usually produces the small and medium size vessel which is made from the wood. The ship will used as the small fishing vessel or as the leisure yacht. According to Deah at al, the traditional shipyard do not have the special place for the production process, sometimes it will located at the riverbank, at the waterfront or behind their house.

Location of the traditional shipyard is usually influence by the geographical factor and material resources. As we know, most of the traditional ship is produces by the wood. To reduce the operation cost, the shipyard is located not far from wood factory where the log was cut into the desired size of wood. The Craftsmen will order the desired quantity of wood form the wood factory based on the specification required by the customer.

The sizes of the shipyard usually not as big as the modern shipyard as they are not produce the traditional ship as a mass production as shown in figure 2. They are only able to build only one of traditional ship depends on the size and specification from customer. They traditional shipyard consist of the Master Craftsmen which will lead as the leader at the ship yard. There was only one or two worker that will help the master in the construction process.

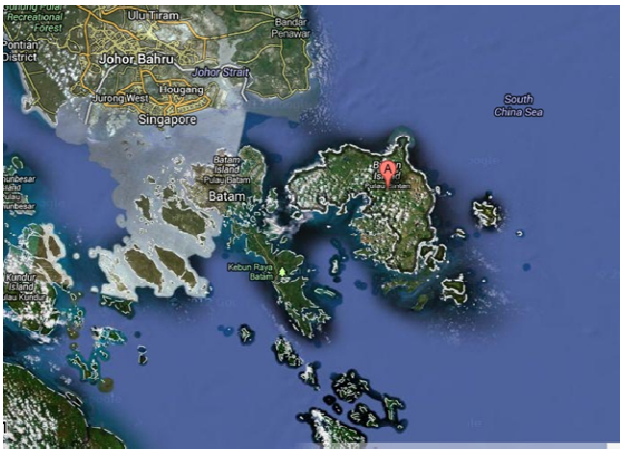

Figure 1: Bintan Islan, Kepulauan Riau, Indonesia. The Bintan Island is surrounded by sea and it is suitable as a shipyard location, source: Google maps.

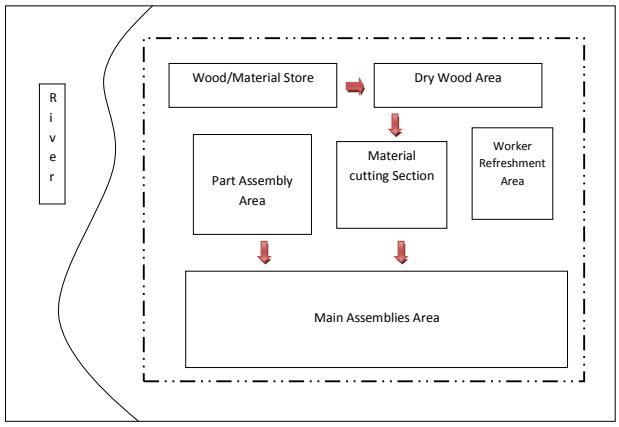

Figure 2: An example of traditional shipyard layout.

In the production process, there are no applications of the big machineries in the ship yard. They are usually used only the small tools such as chainsaw, electric plane hammer and electric borer. All of this small tools and equipment will store at the certain part of the shipyard. As the number of tool applied is less, they are only need a small space compares to the modern shipyard.

Usually a wood that is used in the traditional shipbuilding is seldom available and the masters usually orders in a bulk quantity. They will store the wood at the closed spaced as to avoid the wood to defect and it will affect the quality of the wood. So the traditional shipyards have the specific places to store of the material as shown in the figure 3. Sometimes the woods that send to the traditional shipyard is wet and damps. So to improve the quality of the wood, it must be dry up at the outside of the yard in

order to avoid the wood from easy brittle. This drying process usually took up four months or more so it needs the special space to avoid it block the construction process.

The riverbank and waterfront is the important factor in designing the traditional shipyard as it will help them to launch the ship easily without using the heavy equipment or crane. When the traditional ship is ready for launching, it will directly move up to the river as shown in the figure 4.

Figure 3: Traditional shipyard warehouse

Figure 4: Traditional shipyard at Bintan island located near the river.

3.2 Equipments Used in Indonesian Traditional Shipyards

Manufacturing process of traditional ship in Kepulauan Riau, Indonesia is slightly different from modern ship in the way of building it. All of the process is carried out by human power with the aid of traditional equipment such as saw, chainsaw, electric plane, various sizes of press, blach thread and ruler, electric borer, gauge, nail, bolt, hammer, blorenge and mould as shown in figure 5. The superior of shipyard is called master shipbuilder or master shipwright or master craftsman, is in charged on leading, giving instructions and teaching workers at the yard. The master usually consults his experienced assistant and the ship owner to ensure ability of sailing afterwards and satisfying the owner.

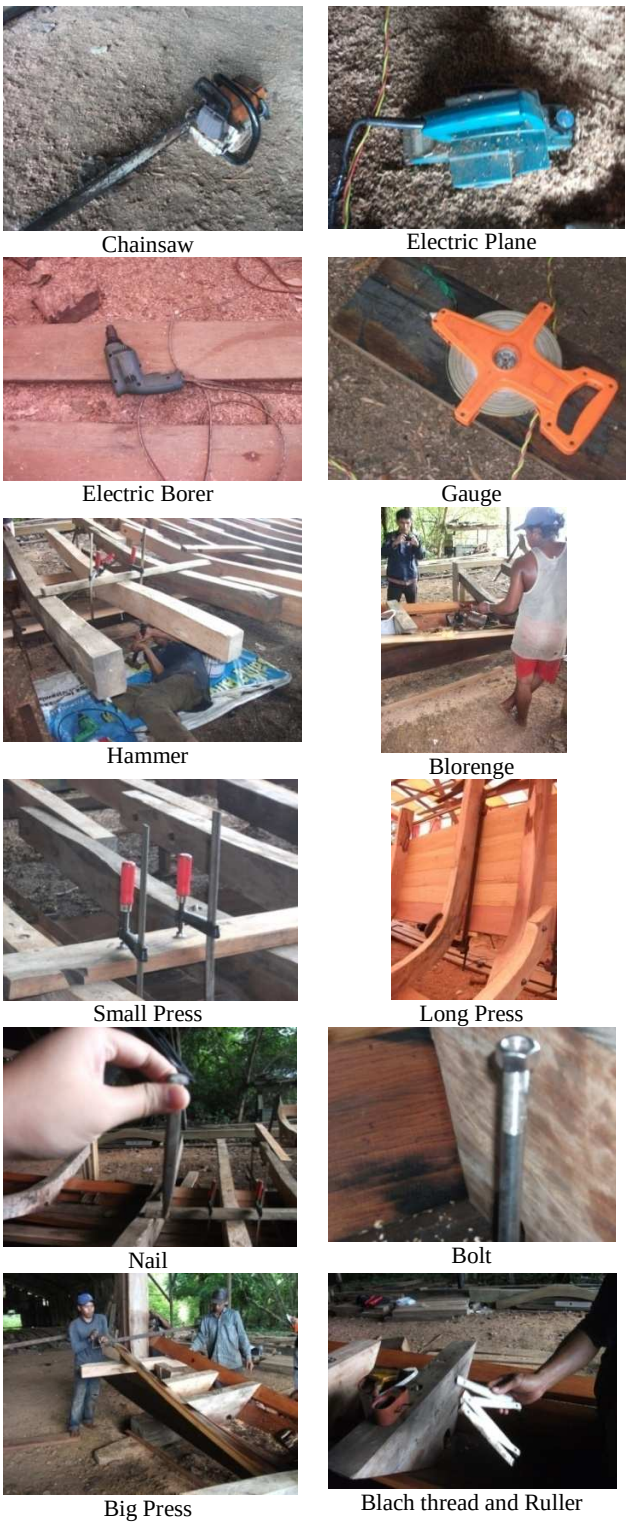

Figure 5: Equipments used in Indonesian traditional shipyards.

4.2 Safety Issues in Ship Production

Each traditional shipbuilder has its own unique way to build a ship. Traditional shipyard in Mana Island used hot bending technique in fastening planks while traditional shipyards in Kijang and Kelong Island were using pressing technique. However, these shipyards has different technique between each other, in general, these shipyards has similarity production process technique to be derived. Figure 6 shows a flowchart of traditional shipbuilding process which is started from contract and payment until delivery.

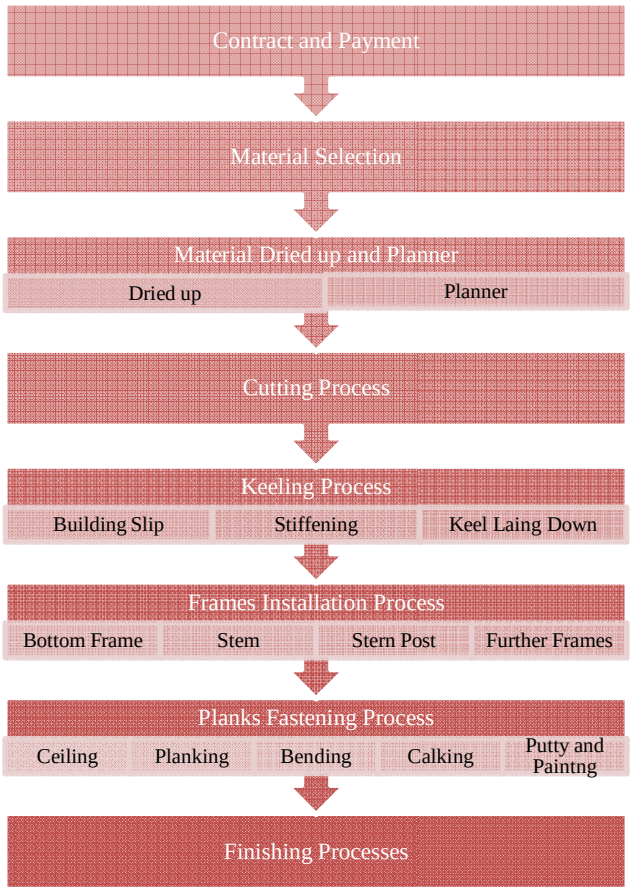

Figure 6: Flowchart of traditional shipbuilding process in Kepulauan Riau-Indonesia.

In traditional ship production process, there is no occupational safety. The shipyard as a protection provider does not recommend or encourage their worker on safety, not even providing personal safety equipment. In figure 7, labor works in unsafe condition and without personal protective equipment as it has regulated on law No.1 1970. As a result, workers are vulnerable to accidents in no time.

Figure 7 shows unsafe condition during working time. There are no effort on accident prevention are taken. The risk such as being squeezed, struck down of wreckage, stepped on nail, direct contact with material, intruding dust in the eyes, and other injury that may occur as a result of non preventing efforts in minimizing accident. In this case, the purpose of occupational safety as a mention by Suma'mur (1993) is not being achieved. If accident would happen, the production and productivity will be disturbed.

Planks are used to cover exterior and interior surfaces of the ribs or frames, and also on the beams of a ship. The skin called as strake is basically a line of planks and named after its position such as garboard strake, sheer strake. The planks fastening process is for upper plank and bottom plank as shown in the figures 8, 9 and 10.

Figure 7: Unsafe condition when cutting the wood.

Shipyard in Mana island used fire bending technique which applying diesel oil and fire to curve and to bend wood into desired form of ship steadily slow as shown in figure 11. Hot bending technique is to deform wood, so that at the time of bending, the wood does not break resulting in easier bending work. To begin with, diesel oil was spread onto the wood as oil base to prevent cracks along the wood which to be shaped. Absorbance of diesel oil will assist in heating the wood thoroughly. Then, the wood would be fired to acquire the curvy shape of a ship hull and then is joined edge to edge using ironwood dowels.

Figure 8: Unsafe condition when hitting a nail in the keel

Figure 9: Planks fastening at bottom frames of ship.

Figure 10: Unsafe condition when planking.

Figure 11: Planks bended using fire technique.

5.0 SUGGESTION AND RECOMMENDATION

All company of construction should be able to serve the worker best personal protection to ensure the safety and the smooth flow of production process. They also should know that any of safety requirements are failed to follow, they are charged on summon and worse, to be jailed for life.

Therefore, in traditional site like there in Kepulauan Riau, the worker should at least wear jacket, boot, glove and face protection such as goggle and mask during work. In the production of traditional ship, they are used to shave wood to create best structure of their ship. Hence, the most practical way to practice safety is to wear glove and goggle. When handling fire, fire extinguisher should always at least 2 meters near to the workers. Workers should wear jacket to prevent fire burn directly on their skin.

6.0 CONCLUSIONS

From description above, it is concluded that safety issue in traditional ship production process is not implemented or not important issue for company and workers as they not applying any safety practice even though occupational safety has regulated on law No.1 1997.

The shortcoming of this study is that safety issue in traditional ship production process are investigated without any comparison between modern ship production process and without make a safety management on traditional ship building company.

The ways of building traditional ships is far from the influence of technology. These would result defects and weakness on the safety for the design and operation. Current research provides the design process in the traditional shipbuilding at Bintan Island, Kepulauan Riau, Indonesia. The result is a comparison to current concept of design process in modern shipbuilding and

recommendation for the traditional shipbuilding and local government. The recommendation is use one of the four ways on the modern shipbuilding or combined from the four ways in order traditional shipbuilding can compete.

ACKNOWLEDGEMENTS

The authors also would like to acknowledge Mr.Akun (Master) and his assistants from Kijang Traditional Shipyard, Mr.Amin (Master) and his assistants from Kelong Island Traditional Shipyard, Master and assistants from Mana Island Traditional Shipyard and warm and grateful thank you to Mr.Hikmat Andi for giving hands, time and fully support for this research.

REFERENCES

1. A.Deah, Jaswar, E.Prayetno, H. Saputra, Mufti F.M, Sanusi, Risandi.D.P, Nofrizal, Zulkarnain, Surhan, and Bayo. (2012), Safety Issue in Production of Traditional Ship in Kepulauan Riau-Indonesia, *The 6th Asia-Pacific Workshop on Marine Hydrodynamics*, pp.571-575.
2. Aji, C. A. (2000). *Local knowledge of traditional boat building by Biak*
3. Adriana, I. (2010). *Occupational Health and Safety*. University of Indonesia Computer: Undergraduate Thesis.
4. Aji, C.A. (2000) *Local Knowledge of Traditional Shipbuilding by Biak Tribe, Sub-Districk of warsa, Districk of Biak Numfor*. University of Cendrawasih: Undergraduate Thesis.
5. Indonesia (1970).*Occupational Health*.: No.1
6. E.Prayetno, Jaswar, H. Saputra, Mufti F.M, Sanusi, A.Deah, Risandi.D.P, Nofrizal, Zulkarnain, Surhan, and Bayo. (2012), Quality Issues in Traditional Ship Production in Kepulauan Riau-Indonesia, *The 6th Asia-Pacific Workshop on Marine Hydrodynamics*, pp.485-489.
7. H. Saputra, Jaswar, Nofrizal, Zulkarnain, E.Prayetno, Mufti F.M, Sanusi, A.Deah, Risandi.D.P, Surhan, Bayo. (2012), Critical Path Analysis of Traditional Ship Production in Kepulauan Riau Indonesia, *The 6th Asia-Pacific Workshop on Marine Hydrodynamics*, pp.571-575.
8. Jaswar and Syafwan bin Anah, 2013, *Traditional Ship Production Case Study in Kepulauan Riau-Indonesia*, Departement of Aeronautic, Automotive and Ocean Engineering, Faculty of Mechanical, Universiti Teknologi Malaysia.
9. Mufti F.M, Jaswar, E.Prayetno, H. Saputra A.Deah, Sanusi, Risandi.D.P, Surhan, Bayo, Nofrizal, Zulkarnain. (2012), Design Issue in Traditional Shipbuilding Process, *The 6th Asia-Pacific Workshop on Marine Hydrodynamics*, pp.565-570.
10. Nofrizal, Zulkarnain, Jaswar, E.Prayetno, H.Saputra, Mufti F.M, Sanusi, A.Deah, Risandi.D.P, Surhan, Bayo, Yasser.M.A, Production Process of Traditional Ships in Kepulauan Riau-Indonesia, *The 6th Asia-Pacific Workshop on Marine Hydrodynamics*, pp.110-117.
11. OHSAS 18001 (2007).Occupational Safety and Health Management System. NCSI Publication
12. Republika (2012). The Number of Indonesia Fisherman Remain Two Million: April 13 2012.
13. Risandi.D.P, Jaswar, Mufti F.M, E.Prayetno, H. Saputra A.Deah, Sanusi, Surhan, Bay, Nofrizal, Zulkarnain. (2012), Planning of Traditional Ship Production in Bintan-Indonesian, *The 6th Asia-Pacific Workshop on Marine Hydrodynamics*, pp.586-589.
14. Simanjuntak, P.J. (1994). *Occupational Safety Management*. Jakarta: HIPSMI
15. Soeprihanto, J. (1996). *Personnel Management*. Yogyakarta: BPPE.
16. Suewedo, H. (2009), *Lingkungan dan Keselamatan Transportasi*: Jurnal Manajemen Mutu. 8(2): 133 – 140.
17. Surhan Jamil Haron, Jaswar, Nofrizal, and Zulkarnain. (2012), Delivery Issues in Malaysian Traditional Ship Production Process, *The 6th Asia-Pacific Workshop on Marine Hydrodynamics*, pp.582-585.
18. Suma'mur. (1993) *Occupational Health and Accident Preventing*. Jakarta: CV Haji Masagung.

Journal of Ocean, Mechanical and Aerospace
-Science and Engineering-, Vol.4

February 20, 2014

Design and Numerical Simulation of Symmetric Multistage Canned Motor Pump

Bin Xia,[a,*] and Fan-Yu Kong,[a]

[a)] *Research Center of Fluid Machinery Engineering and Technology, Jiangsu University, China*

*Corresponding author: xia_bin2007@126.com

Paper History

Received: 1-January-2014
Received in revised form: 5-January-2014
Accepted: 10-January-2014

ABSTRACT

Due to the advantages of high head, no leakage, multistage canned motor pump is widely used in the national economic construction department. At present, in the premise of guarantee reliability, saving energy efficient become an important development direction of canned motor pump. In order to research and improve the performance of the pump, this paper designed and used symmetric multistage canned motor pump DBP15-50x8 as the research object. Three-dimensional model of the main flow passage components is built and the mesh is generated respectively by using Pro/E and ICEM software, and we calculated the whole internal flow field of the pump that was selected by using ANSYS CFX software, achieving the pressure and velocity distribution rule in the pump and the internal details of flow in impeller and other main flow components. It is found that there is pre-whirl flow in the front of inlet in the first stage impeller under the conditions of 0.5 Q and Q flux, obtained the unstableness in inlet when this pump works under the low flux conditions. The post-processing showed the internal flow of bearing section and volute is chaotic, etc. The results provide theoretical basis for the design optimization of multistage canned motor pump.

KEY WORDS: *Symmetrical Type; Multistage; Three-Dimensional Modeling; Structural Design; Numerical Simulation*

1.0 INTRODUCTION

Canned motor pump belongs to no seal pump, the pump and drive motor is enclosed in a pressure contain full of pumped media. Due to the characteristics of multistage canned motor pump can increase the head conveniently, the demand is widely in the water supply and drainage and agricultural engineering, organic chemical industry, aerospace and marine engineering, energy engineering [1-2], however, the development and research of such small flow and high head no leakage pump have a late start, and to this end we have developed a symmetric multistage canned motor pump, then simulated and analyzed it based on CFD software.

2.0 DESIGN

2.1 Hydraulic design

Design performance parameters: Capacity Q=15m3/h, Head H=50m, Rotate speed n = 2900 r/min, Series I = 8. Have hydraulic design according to the parameters. Considering the small inlet pressure and the media easy vaporization, increase imports appropriately to improve the cavitation performance of the first stage impeller, and the design of secondary impeller take the improvement of efficiency as the main consideration. The first stage impeller inlet is 8mm larger than the secondary impellers inlet, and impeller outlet is 0.6mm wider than the secondary impellers. The secondary impeller form drawing is shown in figure 1.

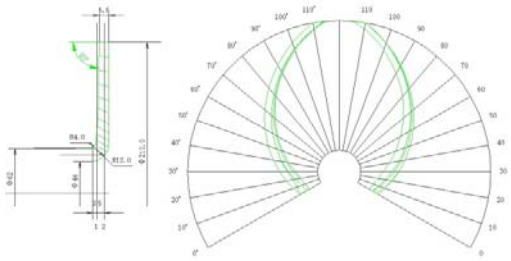

Figure 1: Secondary impellers form drawing.

2.2 Structural design

Multistage canned motor pump adopts symmetrical arrangement structure of four impellers on each side in order to balance axial force mainly. Increase inlet diameter of the first stage impeller to improve cavitation performance, and the other seven impellers have the same basic parameters. Eight impellers symmetrically arranged on both sides of the volute, the first four impellers are counterclockwise rotation from the pump inlet, after four impellers are clockwise rotation. The residual axial force due to other factors at running of pump can be balanced by the thrust plate before and after the canned motor. Symmetric multistage canned motor pump structure shown in figure 2: media inflow after first four impeller, from the water outlet section into the outer cylinder, and then through the water inlet section reverse after four impeller, and finally into the volute and outflow from the outlet.

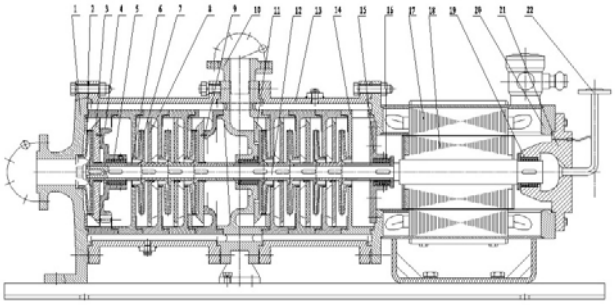

Figure 2: Symmetric multistage canned motor pump structure.
1.Casing cover, 2.The first stage impeller, 3.The first stage guide vanes, 4.Sliding bearing section, 5.Sliding bearing, 6.Shaft sleeve, 7.The secondary stage impeller, 8.Middle section, 9. Water outlet section, 10.Volute, 11.Final stage guide vanes, 12.Shaft, 13.Outer cylinder, 14.Water inlet section, 15.Front bearing housing, 16.Front sliding bearing, 17.Stator, 18.Rotor, 19.Behind sliding bearing, 20.Behind casing cover, 21.Behind bearing housing, 22.The circular tube.

3.0 MODEL OF COMPUTATIONAL MODEL

After the design, Three-dimensional model of the main flow passage components in multistage canned motor pump is built by using Pro/E. We calculated the whole internal flow field of the pump that was selected by using ANSYS CFX software, and analyze the results.

The object of study is the whole internal flow field of multistage canned motor pump, reference to the two-dimensional map of the main flow passage components in multistage canned motor pump, built three-dimensional model of internal flow field by using Pro/E. In the modeling process, in order to prevent the small parts of pump model to affect the quality of the mesh in the mesh generation, leading to inaccurate of numerical calculation, we simplify the model by omitting small gap portion between parts. The three-dimensional model of the internal flow field is shown in figure 3 [3].

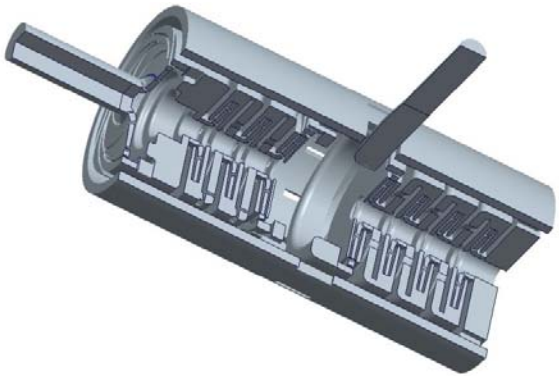

Figure 3: Three-dimensional model of the internal flow field.

4.0 NUMERICAL SIMULATION

In this paper, the internal flow field of multistage canned motor pump is numerical simulated by using ICEM and CFX software.

The entire flow field simulation model including: inlet pipe, the impeller water, the guide vane water, Sliding bearing section water, Middle section water, Water outlet section water, Water inlet section water, volute water and the pipe between outer cylinder and middle section.

4.1 Mesh generation

The reasonable design and high quality of the computational mesh generation is the prerequisite for simulation, also the key factors that affect the simulation. The quality of mesh directly affects the accuracy of the numerical calculation, and even the success or failure of computational problems. This paper used the ICEM to generate mesh. Considering the complexity of the model, we used unstructured mesh for mesh generation. Due to the whole flow field simulation involves many models, the mesh size depends on the size of every model, and the number of mesh after assembly in calculation reached more than 5 million.

4.2 Calculation method

Importing assembled mesh to the flow field calculation of CFX. K-ε turbulence model was selected for the standard model. The mass flow rate outlet and the total pressure inlet were selected for the boundary conditions. The mass flow rate outlet of the whole internal flow field is 15/3.6kg s^-1, the pressure of inlet set at 1 atm. Wall settings according to the domain Settings, the face contact with the rotor parts set to the rotating wall surface, The interface adopts the GGI mesh connection, and the simulation is the unsteady flow situation, the relative motion of the wall set to “Frozen Rotor” option [4-5].

5.0 RESULTS AND ANALYSIS

Figure 4 shows the pressure distribution of the internal flow field in multistage canned motor pump. As can be seen from the figure 4, the pressure increased along the direction of media flow which from the inlet to the outlet.

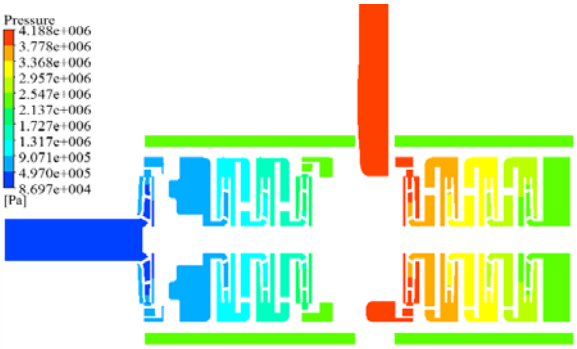

Figure 4: Pressure distribution of the internal flow field.

Figure 5 shows the pressure contours of the level 1, 3 and 7 impeller center plane in multistage canned motor pump. It can be seen from the figure that the pressure from the blade inlet to the outlet increases linearly in three impellers, the pressure near the blade face larger than the pressure near the blade back. From pressure distribution of level 3 and 7 impellers, the pressure in seven secondary impellers are relatively uniform. The pressure near the first stage impeller the pressure face outlet increases faster, showing a high-pressure zone.

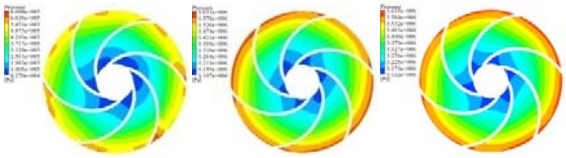

1th stage impeller 3th stage impeller 7th stage impeller

Figure 5: Pressure contours of the level 1, 3 and 7 impeller center plane.

Figure 6 shows the relative velocity contours of the level 1, 3 and 7 impeller center plane in multistage canned motor pump. As can be seen from the figure, the relative velocity increased from the blade inlet to the outlet; the relative velocity in blade back is relatively stable, and increased near the outlet; In the blade face, the relative velocity gradually decreased from blade inlet to the middle of blade, and then gradually increased near the outlet, until closed to the relative velocity in blade back. The relative velocity distribution of secondary impeller is relatively steady, and the work situation of first stage impeller is different from the other seven impellers. There is irregular flow in local areas, the design can be considered separately.

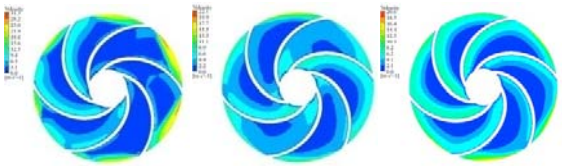

1th stage impeller 3th stage impeller 7th stage impeller

Figure 6: Relative velocity contours of the level 1, 3 and 7 impeller center planes.

Take more planes as the reference surface in multistage canned motor pump, achieving the velocity vector in the flow field by post-processing, and it is shown that the velocity field is uniform in the pump. It proved that the design is reasonable, but there are some places need to improve: Figure 7.a shows the velocity distribution of inlet pipe, It is found that there is pre-whirl flow at the back of inlet pipe obviously under the conditions of 0.5 Q and Q capacity, obtained the unstableness in inlet when this pump works under the low capacity conditions. Figure 7.b shows the velocity distribution in sliding bearing section. The fluid in sliding bearing section rotates around the shaft, but the local flow is chaotic. The existence of the bearing structure leads to a long axial cavity, the media out of the guide vane directly into the bearing cavity. The media have large circumferential velocity, resulting in a movement of rotation around the shaft. The lack of return guide vane lead to irregular flow.

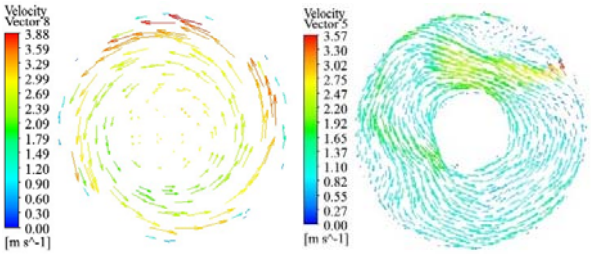

a. inlet pipe b. sliding bearing section

Figure 7: Velocity distribution.

Figure 8 shows the velocity distribution of the volute cross section. The volute as last flow passage components, it can be seen from figure 9 that its flow in some local areas of cavity is chaotic, such as the velocity of 4th cross section is larger than other area around, may cause a large shock loss. It obtained that the volute design is not reasonable. We can further to analyze the results as reference to optimize [6-10].

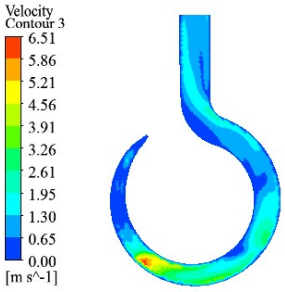

Figure 9: Velocity distribution of volute cross section.

6.0 CONCLUSION

Symmetric multistage canned motor pump is developed to meet the needs of the market for low flow, high head no leakage pump. Impeller arranged symmetrically balances the axial force and reduces the additional balance institutions. Reliability is also improved.

After model and assemble the main flow passage components of pump, this paper simulate the whole internal flow field, more realistic.

Achieving the velocity and the pressure distribution in the flow field by post-processing, the analysis shows that the velocity and the pressure distribution in the flow field are reasonable. The flow of first stage impeller differs from the other seven impellers. It is found that there is pre-whirl flow in the front of inlet in the first stage impeller, the internal flow of bearing section and volute is chaotic, etc. The results provide theoretical basis for the design optimization.

ACKNOWLEDGEMENTS

Special thanks are given to the National Key Technology Support Program entitled "R&D on quickly rescuing drainage equipment during the coal mine flooding process (an amphibious and moving drainage system) (2013BAK06B02)".

REFERENCE

1. Ji JG, Kong FY, Kong XH. Development of the canned motor pump. Pump Technology, 2006, (1) :15-17.
2. Guan XF. Modern Pumps Theory and Design. China astronautic Publishing House, Beijing, China, 2011.
3. Kong FY, Wang T. Rotor dynamic analysis of multistage pump based on numerical simulation of flow field. Journal of Jiangsu University, 2011, 32 (5): 516-521.
4. Wang FJ. Computational fluid dynamics analysis-principle and application of CFD software, Tsinghua university press, Beijing, China, 2004.
5. Liu JR, Zhang LS. CFD numerical simulation of whole flow field for SXB multistage fire pump. Journal of Drainage and Irrigation Machinery Engineering, 2010, 28 (5): 394-397.
6. Zhang XJ. Three-dimensional numerical simulation and performance prediction of multistage pump. Fluid Machinery, 2011, 39 (8): 24-28.
7. Inoue Y, Kimura S, Ono H, et al .Some Performance Predictions for Volute-type Mixed-flow Pump Using CFD [A]. The 7th Asian International Conference on Fluid Machinery [C], Fukuoka, Japan, 2003, 10:7-10.
8. Zhang DS, Shi WD. Hydraulic influence factors and inner flow analysis of centrifugal fire pump. Journal of Drainage and Irrigation Machinery Engineering, 2008, 26(1): 10-14.
9. Tamm and Stoffel. Analysis of a Standard Pump in Reverse Operation Using CFD.20th LAHR Hydraulic Machinery and System, Lausanne, Switzerland, 2002, 10: 20 - 23.
10. Pavesi G, Cavazzini G, Ardizzon G. Time-frequency characterization of rotating instabilities in a centrifugal pump with a vane diffuser. International Journal of Rotating Machinery, 2008, ID: 202179.

Journal of Ocean, Mechanical and Aerospace
-Science and Engineering-, Vol.4

February 20, 2014

Transformation of Directional Wave Spreading in the Surf Zone Using Video Image Data

Muhammad Zikra [a*], Noriaki Hashimoto [b], Masaru Yamashiro [c] and Kojiro Suzuki [d]

[a] *Department of Ocean Engineering, Faculty of Marine Technology, Institut Teknologi Sepuluh Nopember (ITS), Keputih Sukolilo, Surabaya, Indonesia*
[b] *Department of Urban and Environmental Engineering, Faculty of Engineering, Kyushu University, Fukuoka, Kyushu, Japan*
[c] *Department of Urban and Environmental Eng., Faculty of Engineering, Kyushu University, Fukuoka, Kyushu, Japan*
[d] *Marine Environmental Information Group, Port & Airport Research Institute (PARI), Tokyo, Japan*

*Corresponding author: mzikro@oe.its.ac.id

Paper History

Received: 13-January-2014
Received in revised form: 15-January-2014
Accepted: 15-January-2014

ABSTRACT

In present study, video images technique is used to investigate the transformation of the directional wave spreading in shallow water. The technique is based on time series of the pixel brightness on video images. The Bayesian Directional Method is conducted in estimating the directional wave spectrum for evaluating the change of the directional wave spreading in the surf zone area. Video image data recorded at Hasaki beach in Japan are used in the analysis. Estimation of principle direction and spreading parameter in the surf zone regions indicated that principle directions at peak frequency are not strongly affected by wave breaking process. In contrast, the broadenings of directional spreading were observed when the waves start breaking on the sand bar and toward the shore area.

KEY WORDS: *Video Images; Directional Wave Spectra; Principle Direction; Spreading Parameter.*

1.0 INTRODUCTION

Since first developed in 1980, the inventions of new digital technology of images from video camera system have been used and developed into a very useful tool for monitoring coastal changes in the nearshore environment area [1, 2]. After we have successfully extracted wave number components and derived bathymetry in shallow water area with video images data from Hasaki beach in Japan [3], the applicability of video images from Hasaki beach have to be investigated further to study wave characteristic in coastal area.

From previous study showed that wave spectra of pixel brightness on video images at Hasaki site well correspond with the signal of in-situ measurement with the frequency peaks positioned very close to each other [4]. The result indicated that the time series of pixel brightness on video images at Hasaki site containing information about the energy distribution of the wave field which can be used to study wave field in coastal area, in term of its directional wave spectrum.

Despite extensive studies of the shoaling evolution of wave frequency spectra have been done, analysis of the directional wave spectrum has received less attention. In this paper, we analyze the directional spreading function using video images data to study the transformation of the directional spectrum in very shallow water area. Because pixels brightness on video images can be created easily to study the directional spectrum compare to in-situ measurement. The transformations of ocean surface wave across a beach are important to a variety of nearshore processes. The variation of directional spreading function and principle direction for the location inside and outside breaking wave in the surf zone are presented. This research is

conducted with video images data from field measurement on Hasaki beach in Ibaragi prefecture in Japan.

2.0 BASIC THEORY

2.1 The Bayesian Directional Method (BDM)

In this work, the Bayesian Directional Method (BDM), introduced by Hashimoto et al [5] is used to analyze directional wave spreading using video images data. Generally, the BDM provides the highest resolution in estimating the directional wave spectrum. In the BDM, the estimation of a directional wave spectrum can be considered as a regression analysis to find the most suitable model from limited data. The directional spreading function is expressed as a piecewise constant function over each segment of the directional range from 0 to 2π. Since the directional spreading function always greater than or equal to zero, then it can be approximated as

$$G(\theta \mid f) \approx \sum_{k=1}^{K} \exp\{x_k(f)\} I_k(\theta) \tag{1}$$

where

$$I_k(\theta) = \begin{cases} 1: (k-1)\Delta\theta \le \theta < k\Delta\theta \\ 0: \quad \text{otherwise} \end{cases} \tag{2}$$

Generally, the directional spreading function $G(\theta \mid f)$ is assumed a smooth continuous function with respect to the wave direction. This is mathematically expressed by the following relationship between three consecutive values of the estimate.

$$\sum_{k=1}^{K} (x_k - 2x_{k-1} + x_{k-2})^2 \approx 0 \; ; (x_0 = x_K, x_{-1} = x_{K-1}) \tag{3}$$

The optimal estimate of $G(\theta \mid f)$ is obtained by maximize the likelihood function with respect to $\{x_k\}$ within the range where equation (3) does not become too large. These criteria can be formulated using an appropriate parameter u^2. The most suitable value of the hyperparameter u^2 and the estimate of variance σ^2 can be obtained by minimizing the Akaike Bayesian Information Criterion (ABIC) [6] given by:

$$\text{ABIC} = -2\ln \int L(x, \sigma^2) p(x \mid u^2, \sigma^2) dx \tag{4}$$

2.2 Mitsuyasu distribution function

The directional spreading function to be employed in the examination the value of spreading parameter is the following function proposed by Mitsuyasu et al [7].

$$G(\theta) = G_0 \cos^{2s}\left(\frac{\theta - \theta_0}{2}\right) \tag{5}$$

where G_0 is a constant, θ_0 represents the mean wave direction and s represents the spreading parameter. The spreading parameter s can be considered as a parameter which controls the concentration of the directional distribution of the wave energy. The directional distribution tends to a narrower distribution with an increase of the parameter s. The parameter s varies with wave frequency and depends on wave propagation and wave transformation. Goda and Suzuki [8] proposed the following values for s = 10 for wind waves, 25 for swell waves with short decay distance and 75 for swell with long decay distance.

3.0 DATA

3.1 Study Area

This research study was investigated with camera video observation from Hasaki beach in Japan. The Hasaki beach is located on 120 km east of Tokyo facing the North Pacific Ocean as shown in Fig 1. In general, Hasaki beach is known as straight sandy coast stretching from north to south with length around 17 km long. Since 1986, many coastal studies have been conducted in this location especially around the pier which is known as HORS (Hasaki Oceanographical Research Station).

During 2006, the yearly average significant wave height ($H_{1/3}$) is about 1.06 m with corresponding wave period ($T_{1/3}$) of 8.4 seconds. In normal condition, waves approach the coast most often from the East and Southeast directions. The average of the tidal range is about 1.60 m

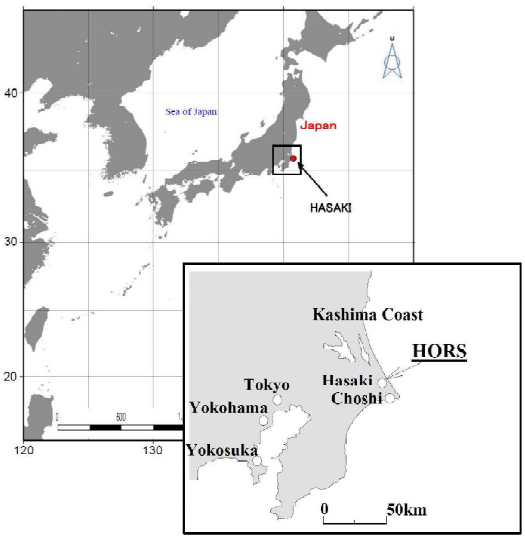

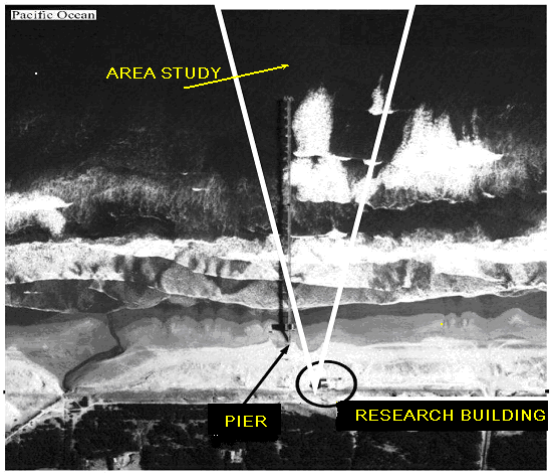

Figure 1: Location of the Hasaki site (top) and aerial photo of the field site (bottom) with the view angle of study area indicated by triangle area

3.2 Data

The actual surface fluctuations in the Hasaki site were recorded using several ultrasonic wave gauges. The ultrasonic wave gauges were installed on the pier with position x = 230 m and x = 145 m from the shoreline. The HORS pier is located at x = 0 m where in-situ wave pressure gauges installed. Water surface fluctuations were recorded as 60 minutes segment, each of which contains approximately 7200 data points, at a sampling rate of 2 Hz.

Meanwhile, image data were collected by using single camera installed in HORS pier at Hasaki beach, Japan in 2006. The digital video camera with the resolution of 640 x 420 pixels was used to acquire snapshot images. This video camera was mounted 10 m high above the ground level. The video images data was recorded for 15 minutes duration at every one hour interval with sampling frequency of 1 Hz. Fig. 2 shows the example of snapshot images recorded by video camera system around pier area at Hasaki site.

3.3 Image Analysis

In order to collect qualitative data, firstly, rectification of the image must be carried out in order to extract quantitative data from a sequence of snapshot images. Rectification involves photogrammetric transformations, which convert image coordinates (u, v) into the real world coordinates (x, y, z) as shown in Fig. 3. This transformation was based on the standard photographic method as described by Holland et al [9].

$$u = \frac{L_1 x + L_2 y + L_3 z + L_4}{L_9 x + L_{10} y + L_{11} z + 1}$$
$$v = \frac{L_5 x + L_6 y + L_7 z + L_8}{L_9 x + L_{10} y + L_{11} z + 1} \quad (6)$$

where the coefficients L1 to L11 are linear functions of the camera orientations (τ, φ, σ), the camera position (x_c, y_c, z_c) and the effective focal length (f), which directly relates to the camera horizontal field of view δ. Three camera orientations, namely the tilt (τ) which represents the rotation with respect to the vertical z-axis, azimuth (φ) which represents the orientation in the horizontal xy-plane and roll (σ) represents of the focal plane with respect to the horizon, respectively.

The inverse transformation from image coordinates to field coordinates results in a system of two equations with three unknowns. The z-coordinates are assumed in this transformation to match a certain horizontal reference level or the tidal water level. Rectified images result from snapshot images is presented in Fig. 4.

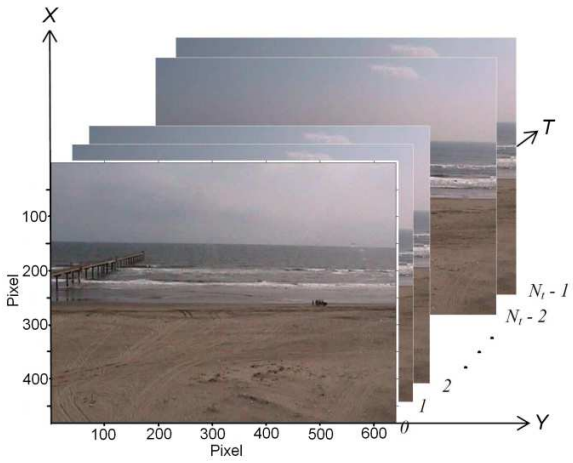

Figure 2: Snapshot image around pier area

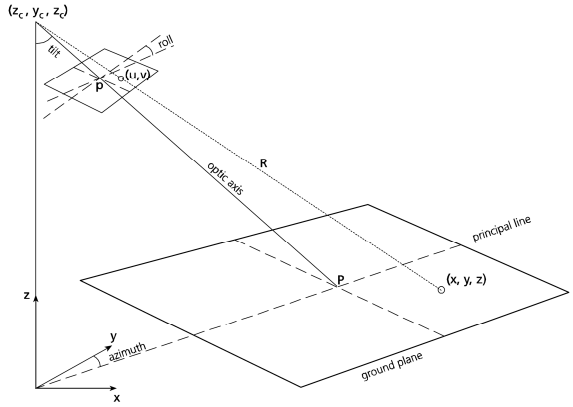

Figure 3: Relation between image coordinate (u, v) and real world coordinate (x, y, z)

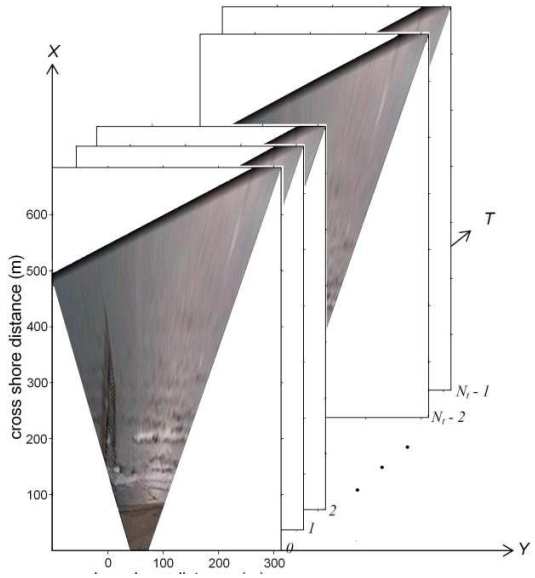

Figure 4: Rectified image time series from snapshot images on 18 August 2006 at 09.00 h around pier area.

4.0 RESULT

In order to study the evolution of the directional spectrum in shallow water, we used video images data recorded on August 18, 2006. In this day, the significant wave height ($H_{1/3}$) was 0.96 m with corresponding wave period ($T_{1/3}$) of 8.2 seconds, and the wave direction was approach from Northeast direction.

Beach profile used in this study were obtained through field measurement and bathymetry inversion using video images (Zikra et al, 2010) as shown in Fig. 5. During August 2006, the crest of sand bar was located approximately 100-120 m from shoreline, causing intense wave breaking at this location. Directional wave spreading were estimated from polygon array of pixel brightness on video images with the distance between pixels, D is 5 m. The location of polygon arrays where the directional spreading observed are shown in A, B, C, D and E label in Fig. 5 below.

The estimated evolutions of directional spreading function across the surf zone regions are plotted in Fig. 6. Meanwhile, the results of mean direction and spreading parameter are tabulated on Table 1. From the Fig. 6, it is observed that outside wave breaking at point A and B, the directional spectrum of swell have a single peak incident spectrum (fp = 0.109 Hz) with a very narrow energy spread in direction and frequency. Also, the wave energy across point A and B resulted nearly constant. Along point A and B, the principle direction, θp is 86^o close to normal incident and the spreading parameter, s is 18.

Table 1 Mean direction and spreading index outside and inside breaking wave.

	Peak frequency, fp	Principle direction, θp	Spreading parameter, s
A.245 m d = 2.3 m	0.109	86	18
B.230 m d = 1.5 m	0.109	86	18
C.215 m d = 1.1 m	0.117	82	6
D.185 m d = 2.0 m	0.101	78	5
E.145 m d = 0.5 m	0.117	86	6

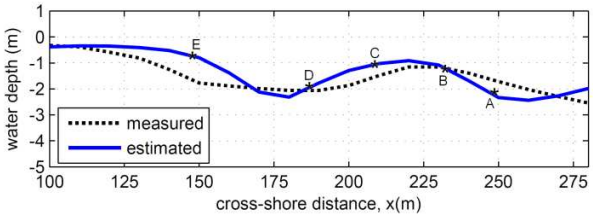

Figure 5: Location of the directional wave spectrum (labeled A, B, C, D, and E) observed along a cross-shore bathymetry profile estimated from video images on August 2006 at Hasaki beach.

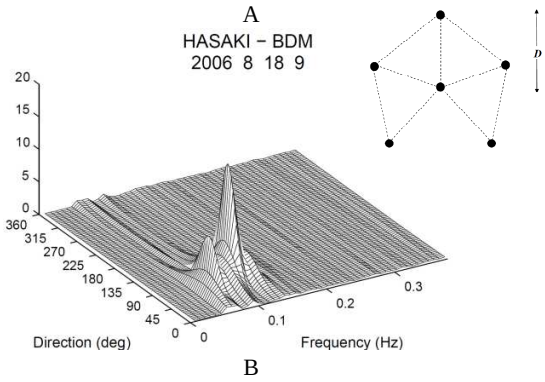

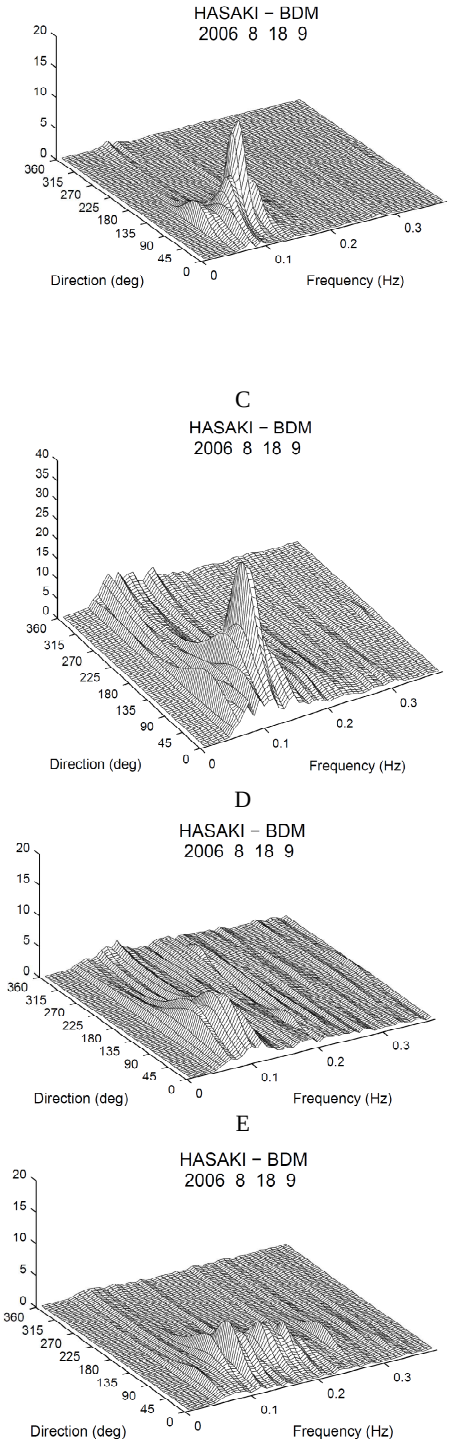

Figure 6: Variation the directional wave spectrum along a cross shore transect on Hasaki beach (insert: polygon array).

On the breaking wave area at point C, the magnitude of wave energy was increased significantly with factor of 2-2.5. As the wave energy increase, the dramatic broadening of directional spreading was observed at peak frequency with the value of spreading parameter decreases sharply from 18 to 6. Also, the principle direction decreases to 82^o from 86^o.

Inside breaking wave area along point D and E, the wave energy decreases significantly toward the shore after breaking. Due to wave breaking, the wave energy was seen gradually spread over a wider range of frequencies. The directional spectra become broader with multiple peaks in the shallower area. In point D and E, directional spreading were observed with spreading parameter 5 and 6, respectively. Meanwhile, the principle direction decreases from 82^o degree to 78^o degree at point D and increasing again to 86^o at the shoreward end of the point E.

5.0 CONCLUSION

This research has been carried out to analyze the variation of directional spreading function and principle direction in shallow water area by using video image data. Video image data recorded at Hasaki beach in Japan were used in the analysis of directional spreading function. The Bayesian Directional Method was conducted in estimating the directional spreading function for evaluating the transformation of the wave directional spectrum inside and outside breaking wave in the surf zone area.

Video images analysis of the estimated evolution of directional spreading in very shallow water area showed that wave breaking does not affect principle directions, θp significantly, but causes the broadening of directional spreading. The value of spreading parameter, s decreased sharply when the waves start entering breaking area. The result indicated that the directional wave spectrum become broader as the wave entering breaking area, suggesting that wave breaking causes directional scattering of wave energy.

Although the results have some uncertainties due to the limitations on the video images technique, as do all measurement methods, the video images method seems a promising technique to understanding the behavior of the wave field in shallow water area and surf zone regions.

ACKNOWLEDGEMENTS

The authors wish to thank Port and Airport Research Institute (PARI), Japan for their data support during this study. Personally, I would also like to acknowledge funding provided by DIKTI, Indonesia during my doctoral study.

REFERENCE

1. Holman, R.A and Stanley, J. (1991): The history and technical capabilities of Argus, *Coastal Engineering*, Vol. 54, pp.477-491.
2. Aarninkhof, S.G. J. and Holman, R. A. (1999): Monitoring the nearshore with video, *Backscatter*, Vol. 10(2), pp.8-11.

3. Zikra, M., Yamashiro, M., Hashimoto, N., and Suzuki, K. (2010): Bathymetry inversion using video image in shallow water, *Annual Journal of Civil Engineering in the Ocean*, JSCE, Vol. 26, pp.1161-1166.
4. Zikra, M., Hashimoto, N., Yamashiro, M., and Suzuki, K. (2011): Spectral analysis of pixel brightness on video images for wave analysis at Hasaki beach, Japan, *CD Room Proceeding of the 21st Int. Offshore and Polar Engineering Conference*.
5. Hashimoto N., K. Kobune and Y. Kameyama. (1987): Estimation of directional spectrum using the Bayesian approach, and its application to field data analysis, *Report of P. H. R. I.*, Vol. 26, No. 5, pp.57-100.
6. Akaike, H. (1980): Likelihood and Bayes procedure, *Bayesian statistics* (Bernardo, J. M., De Groot, M. H., Lindley, D. U. and Smith, A. F. M., eds.) University Press, Valencia, pp.143-166.
7. Mitsuyasu, H., Tasai, F., Suhara, T., Mizuno, S., Ohkusu, M., Honda, T., and Rikiishi, K. (1975): Observation of the directional spectrum of ocean wave using a cloverleaf buoy, *Journal Physical Oceanography*, Vol. 5, pp.750-760.
8. Goda, Y. and Suzuki, Y. (1975): Computation of refraction and diffraction of sea waves with Mitsuyasu directional spectrum, *Technical Note of Port and Harbour Research Institute*, 230, pp.1-45.
9. Holland, K.T, R.A. Holman, T.C. Lipmann, J. Stanley and Plant (1997): Practical use of video imagery in nearshore oceanography, *IEEE J. Oceanic Engineering*, 22(1), pp.81-92.

Head Office

ISOMAse
Resty Menara Hotel
Jalan Sisingamangaraja No.89
28282, Pekanbaru-Riau
INDONESIA
http://www.isomase.org/

ISSN: 2354-7065